

Single-particle electron-tunneling investigation of the phonon spectra and superconductivity of indium-tin alloys

Emery L. Moore, * Robert W. Reed, and F. G. Brickwedde

Department of Physics, The Pennsylvania State University, University Park, Pennsylvania 16802

(Received 15 December 1975)

Single-particle electron tunneling through an oxide barrier, between two metal films, Al-oxide-In_xSn_{1-x}, has been investigated in a study of the lattice and superconducting properties, in particular the phonon density of states, of the four distinct single-phase alloys of the In-Sn system. Measurements of the dynamic resistance of the junction, and second-harmonic response to first-harmonic stimulation across the junction, with the metal films in their superconducting state, have been analyzed using the Eliashberg gap equations and the McMillan computer program. The product function $\alpha^2(\omega_q)F(\omega_q)$, which exhibits the structure of the density of phonon states, $F(\omega_q)$, has been determined for nine intermediate In-Sn compositions. Here $F(\omega_q)$ is the phonon density of states, and $\alpha^2(\omega_q)$ is an electron-phonon coupling parameter which varies slowly with ω_q . In the determination of the phonon spectra, the following normal-state properties of In and Sn, and their alloys have been computed: the Coulomb pseudopotential μ^* ; the electron-phonon interaction strength λ ; and an average phonon energy $\langle\omega_q\rangle$. These three normal-state parameters were used to calculate the superconducting transition temperatures using the McMillan T_c equation. These calculated transition temperatures are compared with our directly measured T_c 's and with previously measured values.

I. INTRODUCTION

For approximately ten years the phenomenon of single-electron tunneling through thin dielectric (oxide) barriers, where at least one side of the barrier is a superconductor, has been yielding considerable new data on the lattice dynamics of strong to intermediate coupling strength superconductors. In particular, the phonon density of states as a function of the phonon energy has been determined for a number of superconducting elements and a few binary-alloy systems. It is the purpose of this paper to present the phonon density of states for four distinct phases, in the In-Sn-alloy system, that differ in composition and structure.

Giaever^{1,2} was the first experimentalist to recognize the usefulness of electron tunneling for obtaining detailed information on the microscopic electron-phonon interaction in superconductors. The use of the tunneling technique has been extended by many workers. The developments leading to the work reported in this paper followed from the theory developed by Schrieffer, Scalapino, and Wilkins³ to explain the experimental data, for tunneling into lead, reported by Rowell, Anderson, and Thomas.⁴ However, it was the work of McMillan and Rowell⁵ in deriving the phonon spectrum of lead from the tunneling data, using the Eliashberg⁶ gap equations, that provided a rather simple method for obtaining the phonon spectra of metals from the tunneling data. Until this development of McMillan and Rowell, the determination of phonon spectra depended on elaborate experimental methods of inelastic neutron scattering.

Fortunately, for the intermediate- to strong-coupling superconductors, for which the tunneling technique is applicable, the tunneling and neutron scattering results complement each other. There is a considerable economy using the tunneling method, but the tunneling method does not yield the dispersion relation $\omega(q)$, which the neutron scattering method does.

The system of In-Sn alloys was selected for investigation for these reasons: First, the end points of the In-Sn compositional spectrum, i.e., pure In and pure Sn, had previously been investigated by the tunneling method^{7,8} and the results were available for comparison. Second, the phase diagram⁹ for the In-Sn binary system, Fig. 1, indicated four different solid-solution phases, with different compositions and structures covering approximately 40 at.% of the compositional spectrum (see Table I), where new information might be obtained. Third, a rather complete investigation by Merriam and von Herzen¹⁰ of the superconducting transition temperatures of these alloys was available for a reasonableness check on some of our results, in particular the compositions of our alloy films. Fourth, it was thought that the vapor pressures of In and Sn were sufficiently alike to permit deposition of alloy films of predetermined composition by the flash-evaporation technique reported by Dynes *et al.*^{11,12}

The theory and technique for deriving phonon spectra from single-electron tunneling into or out of superconductors is given in an extensive review paper by McMillan and Rowell.¹³ The experimental and computational techniques used in this investigation of the In-Sn system are essentially

those of McMillan and Rowell adapted to the conditions in our laboratory. Eleven compositions, including pure In and pure Sn, were investigated. Besides the phonon spectra, we obtained also the density of electron quasiparticles in the superconducting state, the superconducting energy-gap function $\Delta(\omega)$, and the electron-electron Coulomb-interaction term μ^* .

Superconducting transition temperatures T_c of the films were determined by measuring the dynamic resistance of the metal films at zero applied current or voltage bias across the junction, as the temperature was swept through the transition value. The T_c 's were computed, also, using the parameters derived from the tunneling data that characterize the electron-phonon and electron-electron interactions.

II. THEORY

The calculation of phonon spectra from tunneling data using the approach of McMillan and Rowell rests on a refinement of the BCS theory¹⁴ of superconductivity as presented by Eliashberg⁶ and by Nambu.¹⁵ The calculation of superconducting transition temperatures is based also on the Eliashberg-Nambu theory but with some approximations added.

The Eliashberg-Nambu formalism uses a field-theoretical approach treating retardation and damping effects of quasiparticle interactions in a metal. In this formalism (see Schrieffer¹⁶ and Scalapino¹⁷) the superconducting energy-gap parameter at 0 K, $\Delta(\omega)$, where ω is the electron quasiparticle energy ($\hbar=1$), is given by

$$\begin{aligned} \xi(\omega) &= [1 - Z(\omega)] \\ &= \int_{\Delta_0}^{\omega_c} d\omega' \operatorname{Re} \left(\frac{\omega'}{[\omega'^2 - \Delta^2(\omega)]^{1/2}} \right) K_-(\omega, \omega'), \quad (1) \\ \phi(\omega) &= \int_{\Delta_0}^{\omega_c} d\omega' \operatorname{Re} \left(\frac{\Delta(\omega')}{[\omega'^2 - \Delta^2(\omega')]^{1/2}} \right) [K_+(\omega, \omega') - \mu^*], \quad (2) \end{aligned}$$

and

$$\Delta\omega \equiv \phi(\omega)/Z(\omega), \quad (3)$$

where

$$\begin{aligned} K_{\pm}(\omega, \omega') &= \int_0^{\infty} d\omega_q \alpha^2(\omega_q) F(\omega_q) \\ &\times \left(\frac{1}{\omega' + \omega + \omega_q - i\delta} \pm \frac{1}{\omega' - \omega + \omega_q - i\delta} \right) \quad (4) \end{aligned}$$

Here $\xi(\omega)$ is the normal electronic self-energy; $\phi(\omega)$ is the electron-electron pairing self-energy; $Z(\omega)$ is the renormalization function arising from

the electron-phonon interaction; ω_c is a cutoff energy for the integration over electronic energies ω' (ω_c is usually taken to be five to seven times the Debye energy); Δ_0 is the smallest electronic quasiparticle excitation energy for a given temperature (here 0 K); and ω_q is the phonon energy. The Coulomb pseudopotential μ^* was introduced by Morel and Anderson¹⁸ to allow the integral for $\phi(\omega)$ to be terminated at its upper end at ω_c rather than ∞ . $F(\omega_q)$, a function of ω_q , is the phonon density of states. The factor $\alpha^2(\omega_q)$ is an effective electron-phonon coupling function and is a measure of the electron-phonon interaction. $\alpha^2(\omega_q)$ is considered¹⁷ to be a slowly varying function of ω_q which implies that structure in $\alpha^2(\omega_q)F(\omega_q)$ reflects mainly the structure of $F(\omega_q)$. The small effect that $\alpha^2(\omega_q)$ may have on the product $\alpha^2(\omega_q)F(\omega_q)$ has been studied by several workers. Such a study for Pb and $\text{Pb}_{40}\text{Tl}_{60}$ was reported by Rowell, McMillan, and Feldman.¹⁹

McMillan²⁰ devised a way to determine the superconducting transition temperature using a finite-temperature version of the Eliashberg equations.^{21,22} His equation for T_c , often referred to as the McMillan T_c equation, is, as modified by Dynes,⁷

$$T_c = \frac{\langle \omega_q \rangle}{1.2k_B} \exp \left(\frac{-1.04(1+\lambda)}{\lambda - \mu^*(1+0.62\lambda)} \right), \quad (5)$$

where k_B is the Boltzmann constant, and $\langle \omega_q \rangle$ is a weighted average of ω_q defined by

$$A^2 \equiv \int_0^{\infty} \omega_q \left(\frac{\alpha^2(\omega_q)F(\omega_q)}{\omega_q} \right) d\omega_q, \quad (6)$$

$$\lambda \equiv 2 \int_0^{\infty} \left(\frac{\alpha^2(\omega_q)F(\omega_q)}{\omega_q} \right) d\omega_q, \quad (7)$$

$$\langle \omega_q \rangle \equiv \frac{\int_0^{\infty} \omega_q [\alpha^2(\omega_q)F(\omega_q)/\omega_q] d\omega_q}{\int_0^{\infty} [\alpha^2(\omega_q)F(\omega_q)/\omega_q] d\omega_q} \quad (8)$$

$$= \frac{2A^2}{\lambda}. \quad (9)$$

λ is dimensionless, and through its relation to $\alpha^2(\omega_q)$ in Eq. (7) is a measure of the strength of the electron-phonon interaction.

III. EXPERIMENT

Most of the details of instrumentation and processing of data appropriate to this investigation were given by McMillan and Rowell.¹³ Some alterations and additions were necessary to adapt them to our laboratory situation.

A. Junction fabrication and checkout

Several varieties of junction "sandwiches" were investigated; however, all data reported here were

obtained with aluminum-aluminum-oxide-alloy sandwiches. Our use of the term alloy includes pure Sn and pure In as limiting cases. The junctions were evaporated in a vacuum pumped with an oil diffusion pump. The highest vacuum attained was 1×10^{-6} Torr; however, most of the films were evaporated in an initial vacuum of 2 to 4×10^{-6} Torr. The aluminum- and alloy-film strips were evaporated through masks having a slit width of 0.15 mm. Standard 2.5 cm by 7.6 cm microscopic slides were used as substrates. The glass substrate supported a central, lengthwise, aluminum-strip film crossed by three parallel strips of alloy film forming three tunnel junctions. All evaporants were of 99.999% purity. Aluminum wire was cut into small pieces and evaporated from a tungsten canoe boat. The aluminum films were oxidized by plasma oxidation much in the manner discussed by Miles and Smith.²³ Pure oxygen was leaked into the vacuum system, after deposition of the aluminum film, to a pressure of ~ 0.15 Torr. An electrical plasma was established with the negative electrode at ~ -700 V dc relative to the baseplate of the vacuum chamber, which was maintained at ground potential. To obtain junctions with a tunneling resistance of 20–100 Ω , the plasma was continued for 3–6 min. Repeatability in obtaining a given tunneling resistance was enhanced in accordance with Vrba and Woods,²⁴ by keeping a close control on the oxidation current, in our case, a current of 9 mA.

The alloy films were vapor deposited by the flash-evaporation method.⁷ Approximately 75 pellets, about $1 \times 1 \times 1$ mm³ in size, were dropped on a resistively heated tungsten dimple boat. By observing the repeatability of the I , dV/dI , and d^2I/dV^2 vs V traces for several different flash-evaporated junctions derived from the same bulk specimen of an alloy, we were convinced that small pellets flashed from a dimple boat gave repeatably homogeneous films.

After fabrication of a junction, dabs of indium were applied to the ends of the metal films for connecting a junction to a small printed-circuit board which mated with a multipin edge connector. After they were mounted on their circuit boards, the junctions were tested for tunneling resistance at room temperature using a 10 μ A dc current. The second-harmonic-detection circuit, to be discussed below, was a tuned reactive network, which performed best for junctions having tunneling resistances in the range 20–100 Ω . Junctions with tunneling resistances outside the prescribed range were not used for phonon-spectrum calculations. Confirmation that the resistance measured at room temperature was true tunneling resistance as distinguished from simple Ohmic resistance

in the oxide layer, was achieved by observing the I - V trace of the junction below its superconducting transition temperature. Further criteria applied for selection of tunnel junctions were based on the criteria outlined by McMillan and Rowell.¹³

B. Instrumentation

Four kinds of experimental data were needed for determining the phonon spectra. These were: (a) Δ_0 (obtained from the I vs V trace of the junction at $T \rightarrow 0$ K); (b) and (c) the conductances, dI/dV , vs V of the junction when both metal films were in their (i) superconducting and (ii) normal states; and (d) the second-harmonic response, $e(2\omega_0)$, vs V , of the junction to a first-harmonic stimulus, $e(\omega_0)$, when the metal films were in their superconducting state. $e(2\omega_0)$ is directly related [see Eq. (10)] to d^2I/dV^2 . All the indicated measurements in the superconducting state were made at 1 K. The normal state was established at 2 K with a magnetic field of ~ 3 kOe. To verify that the normal state was achieved using the 3-kOe field, the conductances of some junctions thus obtained were checked in zero magnetic field at temperatures a little higher than T_c .

The bridge circuit of Adler and Jackson²⁵ (excited at 1.45 kHz) was adapted for the measurement of the conductances dI/dV vs V , but it was used here without the filters employed by Adler and Jackson. As a result a small second-harmonic signal, originating as oscillator distortion, was present in the circuit and prevented our use of the circuit for the measurement of the second-harmonic response of the tunnel junction. The second-harmonic signal was obtained using the circuit of Thomas and Rowell.²⁶ Because of its highly tuned filter networks, it was necessary to restrict the choice of acceptable tunneling resistances to the range 20–100 Ω . The signal levels of interest in the second-harmonic response were of the order of several nanovolts. Hebard and Shumate²⁷ reported a circuit using two lock-in amplifiers for measuring both the conductances and the second-harmonic response, that will accommodate junction resistances from 1 to 10^4 Ω .

Transition temperatures T_c were determined by the sensitive method of Feldman and Rowell.²⁸ This method makes use of the same circuit used for measurements of the conductance except that no dc current bias is used. The tunnel resistance dV/dI measured with the junction excited by a small ac current, was plotted with an X-Y recorder as a function of the voltage across a calibrated Ge resistance thermometer carrying a 1- μ A constant current.

C. Data processing

This section is a brief outline of the computation procedures for extracting the density of phonon states $\alpha^2(\omega_q)F(\omega_q)$ from the experimental data, and in the process obtaining the gap function $\Delta(\omega)$; the density of quasiparticle electron states $N_{Ts}(\omega)$ in the superconducting state; and the Coulomb-interaction term μ^* . The experimental data consist of (i) the dynamic resistances dV/dI of the junctions as functions of V when both metal films are either superconducting or normally resisting, (ii) the second-harmonic response $e(2\omega_0)$ of the tunnel junction to first-harmonic stimulation when the metal films are superconducting, and (iii) Δ_0 , the superconducting gap parameter at $T \rightarrow 0$ K. The calculation followed that of McMillan and Rowell.¹³ Their computer program was used with necessary adaptations to special conditions of the laboratory. Thus, for example, the dynamic resistance and second-harmonic data were tape punched at equal intervals of time, whereas McMillan's program processes these data at equal intervals of junction bias voltage. McMillan's program is described in a University of Illinois technical report by Hubin.²⁹

The second-harmonic response $e(2\omega_0)$ and the conductivity σ_s of the junction are related functions of V , when both metal films are superconducting. Using the circuit of Thomas and Rowell²⁶ this relation is

$$\begin{aligned} \frac{d\sigma_s}{dV} &= \frac{d}{dV} \left(\frac{dI}{dV} \right)_s = \left(\frac{d^2I}{dV^2} \right)_s \\ &= \frac{e(2\omega_0)}{e_A(\omega_0)} (K_1 + K_2\sigma_s + K_3\sigma_s^2 + K_4\sigma_s^3), \end{aligned} \quad (10)$$

where the K_i 's are constants, determined by constants for circuit elements, and $e_A(\omega_0)$ is the amplitude of the fundamental exciting signal $e(\omega_0)$. Dropping terms in σ_s^n of higher order than the first was justified since only junctions with $\sigma_s < 0.05$ mho were used. By integrating Eq. (10) and dividing by the slowly varying function σ_n , $(dV/dI)_n^{-1}$, the experimental conductance and second-harmonic data (Figs. 2-5) were combined in

$$\left(\frac{\sigma_s}{\sigma_n} \right)_f \equiv A \int e(2\omega_0) dV + B \int e(2\omega_0) \left(\frac{\sigma_s}{\sigma_n} \right)_e dV + CV + D \quad (11)$$

where A , B , C , D are constants whose values were determined by making a least-squares fit of $(\sigma_s/\sigma_n)_f$ to the experimental data $(\sigma_s/\sigma_n)_e$ obtained from the superconducting and normal state dynamic resistance traces. The last two terms of Eq. (11) were added to absorb all constant and linear effects overlooked in previous approxi-

mations; e.g., absorption into the constant factor A of the function σ_n which should appear in the denominator of the first term on the right-hand side of Eq. (11). The $(\sigma_s/\sigma_n)_f$ data were "smoothed" in accordance with

$$\left(\frac{\sigma_s}{\sigma_n} \right)_{SM} \equiv \left(\frac{\sigma_s}{\sigma_n} \right)_f + \int_{V-\Delta V}^{V+\Delta V} dV' \left[\left(\frac{\sigma_s}{\sigma_n} \right)_e - \left(\frac{\sigma_s}{\sigma_n} \right)_f \right] f(V, V'), \quad (12)$$

where $f(V, V')$ is a weighting function of Gaussian form:

$$f(V, V') \equiv \frac{\exp[-(V' - V)^2/2\sigma_{SM}^2]}{\int_{V-\Delta V}^{V+\Delta V} dV' \exp[-(V' - V)^2/2\sigma_{SM}^2]}. \quad (13)$$

A ΔV equal to 0.9 mV was used for the In-Sn alloys along with a standard deviation σ_{SM} equal to 0.2-0.3 mV.

The $(\sigma_s/\sigma_n)_{SM}$ data were used to calculate our experimental results for the normalized electronic quasiparticle tunneling densities of states, $N_{Ts}(\omega)/N_{Tn}(0)$, of the alloy films. The McMillan program was used to deconvolute

$$\left(\frac{\sigma_s}{\sigma_n} \right)_{SM} = \frac{d}{dV} \int_0^V \frac{N_{Tsa}(\omega)}{N_{Tna}(0)} \frac{N_{Tsb}(V-\omega)}{N_{Tnb}(0)} d\omega, \quad (14)$$

where the subscripts a and b represent the two metal films of the junction. In Eq. (14) the factor $N_{Ts}(\omega)/N_{Tn}(0)$ for either metal a or b is the energy-dependent quasiparticle density of states in the superconducting state. It is normalized by the quasiparticle density of states in the normal state measured at the Fermi level. Equation (14) was first suggested by Giaever and can be found as Eq. (55) in Ref. 13. Since all our junctions had Al for one film, and since Al is a weakly electron-phonon-coupled superconductor, we were justified, as McMillan and Rowell observed, in using the BCS density-of-states function in Eq. (14) for one metal:

$$\frac{N_{Ts, Al}(V-\omega)}{N_{Tn, Al}(0)} = \frac{V-\omega}{[(V-\omega)^2 - \Delta_0^2]^{1/2}}. \quad (15)$$

The value of $\Delta_0(\text{Al})$ was determined for each junction from the junction's $I-V$ trace.

The phonon spectra, $\alpha^2(\omega_q)F(\omega_q)$ (Fig. 8) were derived from the electron density of states, $N_{Tsa}(\omega)/N_{Tna}(0)$, which represented the experimental data. The superconducting gap function $\Delta(\omega)^{(1)}$, Eq. (3), was calculated using the Eliashberg Eqs. (1)-(4), in an inverted manner starting with initially assumed functions $[\alpha^2(\omega_q)F(\omega_q)]^{(0)}$ and $\Delta(\omega)^{(0)}$. This calculation made use of the McMillan program. The calculated $\Delta(\omega)^{(1)}$ was substituted for $\Delta(\omega)$ in Eqs. (1) and (2) and the calculation was repeated yielding $\Delta(\omega)^{(2)}$, which was again substituted for $\Delta(\omega)$ in Eqs. (1) and (2). The calculation was iterated (four or five

times were sufficient) until Eq. (3) yielded essentially the same function for $\Delta(\omega)^{(1)}$ as was substituted in the Eliashberg Eqs. (1) and (2). With this function $\Delta(\omega)^{(1)}$, the calculated density of electron quasiparticle states was obtained^{16,30}:

$$\left(\frac{N_{Tsa}(\omega)}{N_{Tna}(0)}\right)_c \equiv \text{Re} \left(\frac{\omega}{[\omega^2 - \Delta^2(\omega)^{(1)}]^{1/2}} \right). \quad (16)$$

$[N_{Tsa}(\omega)/N_{Tna}(0)]_c$ was compared with the experimentally derived $[N_{Tsa}(\omega)/N_{Tna}(0)]_e$ obtained using Eq. (14) and an adjustment was made to the initial guess for $[\alpha^2(\omega_q)F(\omega_q)]^{(0)}$. Another solution was obtained for $[N_{Tsa}(\omega)/N_{Tna}(0)]_c$, Eq. (16), which more closely resembled the empirical $[N_{Tsa}(\omega)/N_{Tna}(0)]_e$ if $(\alpha^2F)^{(0)}$ was adjusted correctly. The process was iterated (usually four or five iterations were sufficient) until $[N_{Tsa}(\omega)/N_{Tna}(0)]_c$ closely resembled $[N_{Tsa}(\omega)/N_{Tna}(0)]_e$. A function was thus obtained for $\alpha^2(\omega_q)F(\omega_q)$, Fig. 8, which yielded for $[N_{Tsa}(\omega)/N_{Tna}(0)]_c$ a result that was essentially identical with the empirical $[N_{Tsa}(\omega)/N_{Tna}(0)]_e$.

Agreement of the calculated and computed densities of quasiparticle states could be forced as closely as desired by further iterations of the program. For each of our alloys no visible change could be seen in the plots of the $\alpha^2(\omega_q)F(\omega_q)$ function beyond five iterations of this process. Further iterations reproduced the $\alpha^2(\omega_q)F(\omega_q)$ spectral phonon curve entered in the program. A demonstration that the Eliashberg equations, as employed in the McMillan program, accurately predict experimental reality was shown in a test-experiment reported on pp. 607-609 of the paper by McMillan and Rowell.¹³ In this experiment a phonon spectrum was obtained for Pb by computing a quasiparticle density of states in agreement with the experimentally derived density of states for energies below 11 meV. The phonon spectrum thus obtained was used to predict the Pb quasiparticle density of states normalized to the BCS density of states in the energy interval between 11 and 27 meV. The predicted normalized density of states was shown to agree with its experimental counterpart to within ± 0.001 . This figure can be compared with 0.07, the maximum deviation from unity of the Pb density of states normalized with the BCS density of states. Comparing 0.001 with 0.07 gives an "accuracy" for this test-experiment of approximately 1.4%, conclusive evidence of the precise nature of the Eliashberg theory as implemented via the McMillan program.

In the iteration of the computation, it was necessary to compute in addition to the phonon spectra a number of meaningful quantities. These were the renormalization function $Z(\omega)$; the pairing self-energy $\phi(\omega)$; the gap function $\Delta(\omega)$, Figs. 9 and 10; and the Coulomb pseudopotential μ^* , Table II.

All were printed out following computation. A compilation of these results is available from the Department of Physics at The Pennsylvania State University. The renormalization function for the *normal state* of the metal was computed by letting $\Delta(\omega)$ be zero. The Coulomb pseudopotential μ^* , a normal state property, was adjusted at each iteration so that the computed value of $\Delta(\omega)$ at $\omega = \Delta_0$ was Δ_0 [i.e., $\Delta(\Delta_0) = \Delta_0$]. It was necessary to provide the program with an initial estimate of μ^* . A value of 0.11, representative of the theoretical Coulomb pseudopotential for Pb, was used for an initial estimate.

IV. EXPERIMENTAL DATA AND CALCULATED RESULTS

A. Conductance data and electronic quasiparticle density of states

Eleven In-Sn alloys, including pure In and pure Sn, as limiting members of the alloy system, were investigated and their phonon spectra $\alpha^2(\omega_q)F(\omega_q)$, Fig. 8, were derived. The solid alloy system consists of four structurally and compositionally distinct single phases. They are designated In-like, β , γ , and Sn-like. Composition ranges (in at.%) of single-phase regions at 300 K are given in Table I. See also Fig. 1.

The quasiparticle density of states was derived from the measurements of the dynamic tunneling resistance and the second-harmonic response of the junction, related to $(d^2I/dV^2)_s$, see Eq. (10). Figures 2 and 3 are examples of the raw data traces of the dynamic tunneling resistance for the β and γ phases, respectively, in the In-Sn-alloy system in both the superconducting and normal states. The β phase is represented by the data for an Al-I-In_{0.79}Sn_{0.21} tunnel junction and the γ phase by data for an Al-I-In_{0.16}Sn_{0.84} junction. Compositions are in at.%. Data are given for both the superconducting state (solid line) and the normal state (dashed line).

Figures 4 and 5 are examples of the second-harmonic traces for the β and γ phases, respectively. They were obtained for the same junctions that produced Figs. 2 and 3. The scaling on the ordinate axis for the second-harmonic traces represents full-scale sensitivity of the detection system. Actual scaling was determined by a fit to the dynamic resistance traces as discussed in Sec. III C, see Eq. (11). Note that peaks (maxima) in the second-harmonic trace for a given junction correspond with inflections from negative to positive curvature in the dynamic resistance trace.

The dynamic resistance and second-harmonic response traces for pure-In and pure-Sn junctions are representative of the indium (In) and tin (Sn) terminal phases of the In-Sn-alloy system. Sec-

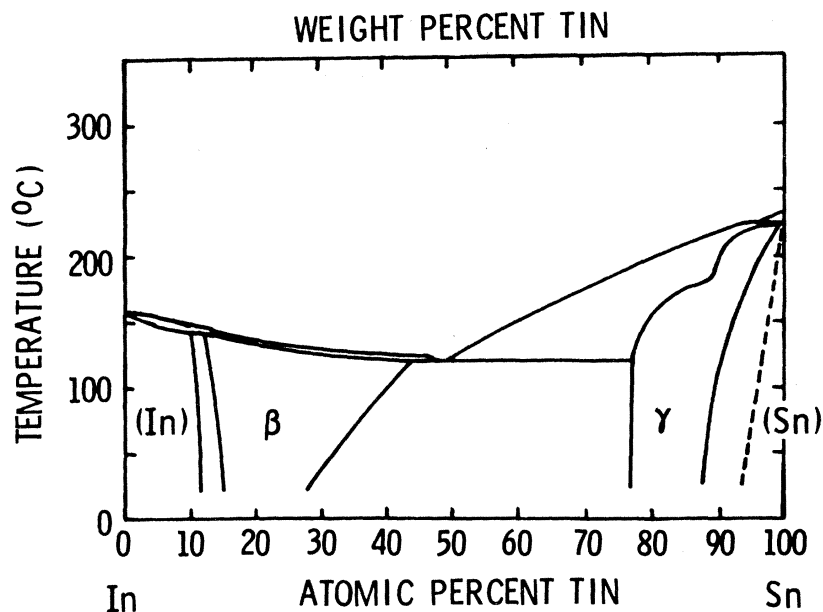


FIG. 1. Phase diagram for the In-Sn binary system from Ref. 9.

ond-harmonic and dynamic resistance data for pure In were reported by Rowell, McMillan, and Dynes,³² and for pure Sn by Rowell, McMillan, and Feldman.⁸ Our results for pure In and pure Sn are in close agreement with these previous measurements and are not reported here. Our data for the In-Sn binary alloys are, as far as we are aware, original.

In the McMillan computer program for the calculation of the electron density of states [see Sec. III C and Eq. (14)] the assumption was made that Al has a BCS density of states. The BCS density is based on the assumption that the pairing inter-

TABLE I. Crystal structure of solid-solution phases of the In-Sn-alloy system at ~ 300 K.^a

Phase	Lattice type	Composition (at.% Sn)	Lattice dimensions (~ 300 K)		
			a (Å)	c (Å)	c/a
(In)	bct (H, W ^b)	0.0	3.244	4.938	1.522
		9.6	3.227	5.020	1.556
β	bct (P ^b)	14.47	3.431	4.451	1.297
		28.49	3.474	4.358	1.254
γ	hex (H ^b)	77.66	3.216	2.998	0.932
		89.65	3.221	3.000	0.931
(Sn)	tet (H ^b)	94.8	5.828	3.182	0.546
		100.0	5.831	3.181	0.546

^a Phase in Col. 1, with structure in Col. 2, exists between upper and lower compositions in Col. 3.

^b Data from H-Hansen (Ref. 35); W-Wyckoff (Ref. 39); and P-Pearson (Ref. 40).

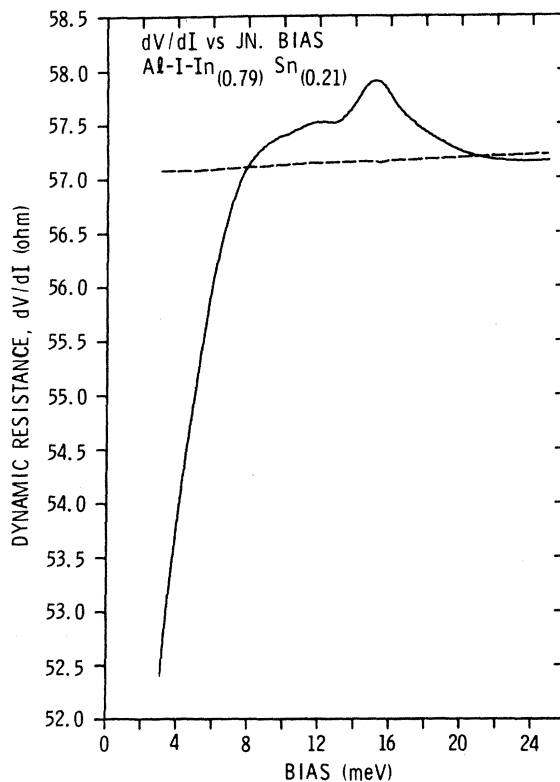


FIG. 2. Dynamic resistance dV/dI for an Al-I- $\text{In}_{0.79}\text{Sn}_{0.21}$ junction, representative of the β phase of the In-Sn system. The superconducting trace at 1 K is given by the solid line and the normal state-trace at 1 K by the dashed line.

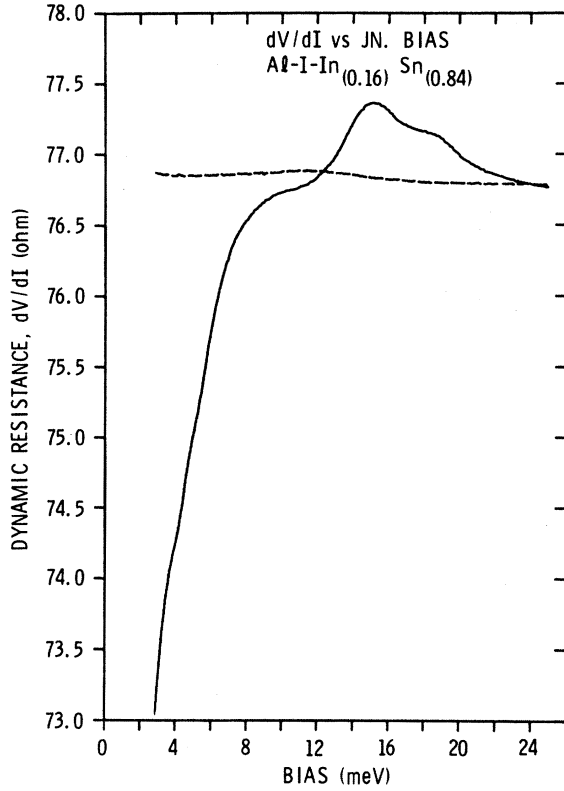


FIG. 3. Dynamic resistance dV/dI for an Al-I-In_{0.16}Sn_{0.84} junction, representative of the γ phase of the In-Sn system. The superconducting trace at 1 K is given by the solid line and the normal-state trace at 1 K by the dashed line.

action of electrons is a constant for all electrons having energies within the Debye energy ω_D of the Fermi surface. An assumed (BCS) density of states for Al was used to remove the effect of the Al from the experimental data and give the electronic density of states $N_{Ts}(\omega)$ of the metal of in-

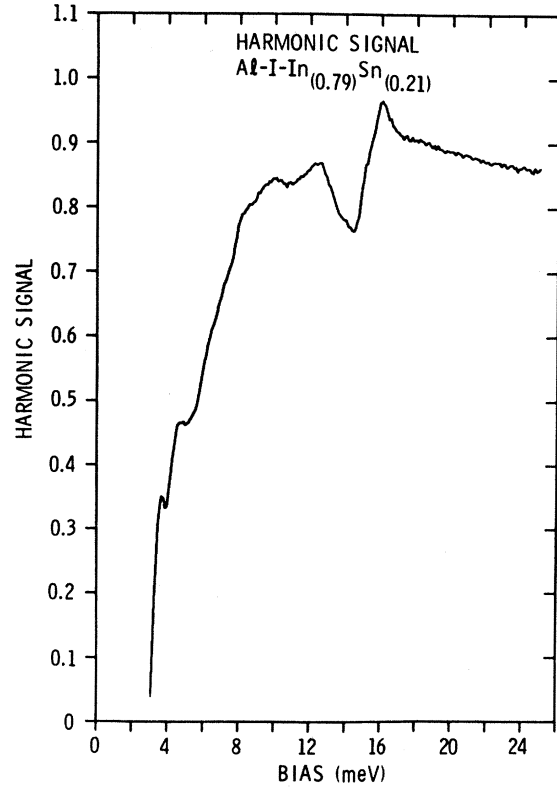


FIG. 4. Second-harmonic trace $e(2\omega_0)$ (roughly d^2I/dV^2) for an Al-I-In_{0.79}Sn_{0.21} junction, representative of the β phase of the In-Sn system at 1 K.

terest.

A BCS density of states was computed for each of the In-Sn alloys using the experimentally determined (from the $I-V$ trace) Δ_0 's. The experimental Δ_0 's are listed in Table II. Figures 6 and 7 are graphs of the ratios of the electron density of states $N_{Ts}(\omega)$ [i.e., $N_{Ts}(\omega)/N_{Tn}(0)$] to the BCS density of states for our representatives of the β -

TABLE II. Experimentally derived superconductivity parameters for single-phase In-Sn alloys.

Composition (at.%)	Alloy phase	Δ_0 (meV)	μ^*	A^2 , Eq. (6) (meV)	λ , Eq. (7)	$\langle\omega_q\rangle$, Eq. (8) (meV)	T_c (tun) (K)	T_c (M, vH) ^a (K)	T_c (McM) ^b (K)
In	(In)	0.549	0.140	2.91	0.853	6.82	3.47	3.40	3.23
In _{0.95} Sn _{0.05}	(In)	0.578	0.122	2.84	0.845	6.72	3.67	3.86	3.53
In _{0.91} Sn _{0.09}	(In)	0.635	0.137	3.08	0.932	6.61	4.00	4.40	3.86
In _{0.89} Sn _{0.17}	β	0.835	0.102	3.29	1.04	6.33	...	5.48	5.38
In _{0.79} Sn _{0.21}	β	0.930	0.121	3.59	1.16	6.19	...	5.77	5.65
In _{0.75} Sn _{0.25}	β	0.980	0.108	3.56	1.16	6.14	...	6.02	5.92
In _{0.20} Sn _{0.80}	γ	0.685	0.144	3.76	0.939	8.01	4.40	4.41	4.55
In _{0.16} Sn _{0.84}	γ	0.725	0.146	3.79	0.940	8.06	4.50	4.74	4.53
In _{0.14} Sn _{0.86}	γ	0.720	0.163	3.77	1.07	7.05	4.78	4.84	4.61
In _{0.05} Sn _{0.95}	(Sn)	0.580	0.140	3.55	0.838	8.47	3.78	3.69	3.85
Sn	(Sn)	0.595	0.158	3.72	0.862	8.63	3.74	3.69	3.66

^a M, Merriam; vH, von Herzen.

^b McM, McMillan.

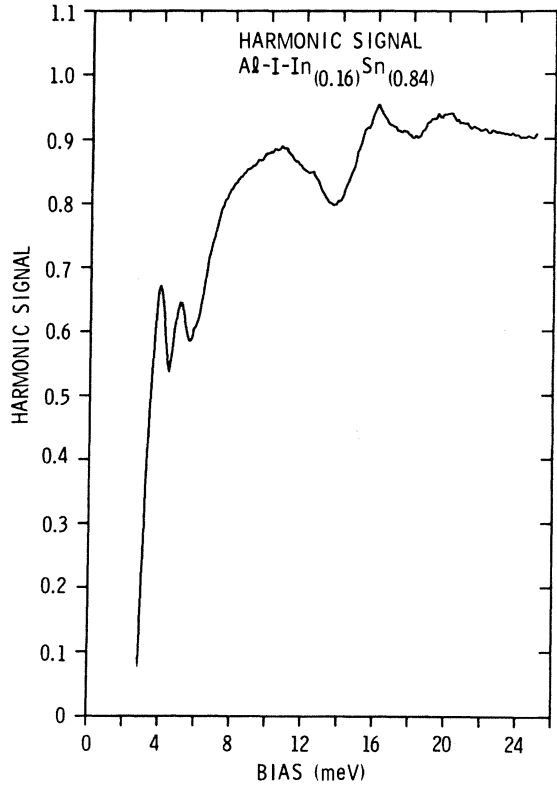


FIG. 5. Second-harmonic trace $e(2\omega_0)$ (roughly d^2I/dV^2) for an Al-I-In_{0.16}Sn_{0.84} junction, representative of the γ phase of the In-Sn system at 1 K.

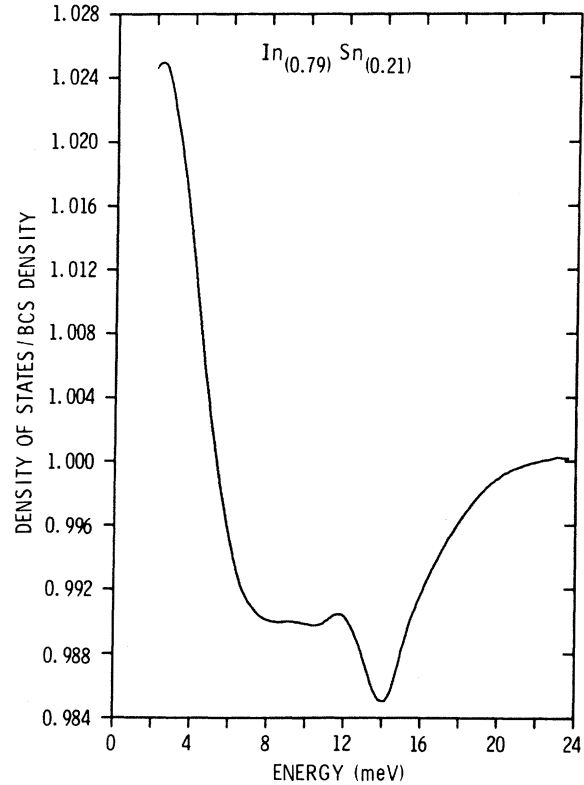


FIG. 6. Superconducting electronic density of states divided by the BCS density of states, $N_{Ts}(\omega)/N_{TBCS}(\omega)$, for an Al-I-In_{0.79}Sn_{0.21} junction representative of the β phase of the In-Sn system.

and γ -phase alloys: In_{0.79}Sn_{0.21} and In_{0.16}Sn_{0.84}. These are sensitive representations of the departures of $N_{Ts}(\omega)$ from BCS theory. Structure in these graphs indicates the influence of the phonon spectra on the pairing interactions and subsequently on the electronic quasiparticle density of states. Comparing Figs. 6 and 7 with the corresponding phonon spectra, $\alpha^2(\omega_q)F(\omega_q)$, in Fig. 8 it will be seen that "drops" in the functions of Figs. 6 and 7 can be associated with peaks in the corresponding phonon spectra. The electronic density of states have previously been reported for pure In,^{33,34} and for pure Sn.⁸ Our results are in very good agreement with these earlier results for both In and Sn.

A way to determine errors in a mathematical solution as complex as the McMillan program is to run the McMillan solution on data gathered from several tunnel junctions using the same metal of interest. Rowell *et al.*,⁸ following this procedure for five different Sn junctions, determined that typical error bars for density-of-states ratios, such as those shown in Figs. 6 and 7, spanned a range of 0.001. For energies below approximately 3 meV, where closeness to the gap

increased error sensitivity, an error bar spanning a range of 0.0015 appeared more appropriate.

B. Gap-equation results

Using the Eliashberg gap equations (1)–(4), the McMillan computer program derived the phonon density-of-state functions $\alpha^2(\omega_q)F(\omega_q)$ for the eleven different alloys in Fig. 8 from their experimentally determined densities of electronic quasiparticle states (see Sec. IIIC). The product function $\alpha^2(\omega_q)F(\omega_q)$ is dimensionless since $\alpha^2(\omega_q)$ has the dimension of energy and $F(\omega_q)$ has the dimension of the reciprocal of energy.

The four single-phase solid-solution alloys of the In-Sn system are represented in Fig. 8. Three of these four phases have tetragonal lattice structures. These are the (In) phase (top three traces), the β phase (fourth, fifth, and sixth traces), and the (Sn) phase (the bottom two traces). The γ phase (seventh, eighth, and ninth traces) has a hexagonal structure.³⁵

The spectra for the (In) and (Sn) phases are well represented by the spectra for pure In and pure Sn. Spectra for the (In) and β phases are similar,

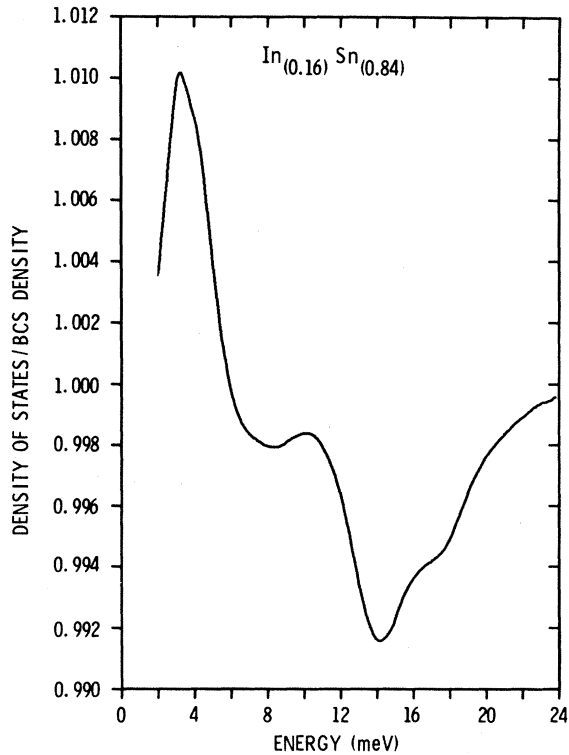


FIG. 7. Superconducting electronic density of states divided by the BCS density of states, $N_{TS}(\omega)/N_{TBCS}(\omega)$, for an Al-I-In_{0.16}Sn_{0.84} junction representative of the γ phase of the In-Sn system.

however, there is a progressive shift to lower energies of the low-energy maximum (at ~ 6 meV) in the spectra as the Sn content is increased. The spectra of the (In)- and β -phase alloys terminate, at their high-energy end, at about 16 and 15.5 meV, respectively, whereas the spectra for the γ and (Sn) phases terminate at about 19.0 and 18.0 meV. A distinctive feature of the spectra for the γ phase is the broad band of intermediate and roughly uniform intensity between 15 and 18 meV. Possibly, the smaller lattice dimension of the γ phase, as compared with that for the (In) and β phases, may be associated with the appearance of this band of states between 15 and 18 meV.

The general shape of the γ -phase spectrum is similar to that found by Shen³⁶ for Nb₃Sn. Dynes⁷ indicates that hexagonal lattices typically show a "strong low-energy peak," a characteristic that is not apparent in the three γ -phase spectra in Fig. 8. Shen did not specify the lattice structure corresponding to his Nb₃Sn phonon spectrum. Nb₃Sn exhibits both a cubic and a tetragonal structure.³⁷ There may therefore be some reason to question whether the hexagonal structure attributed to the γ phase persists at low temperatures. Our

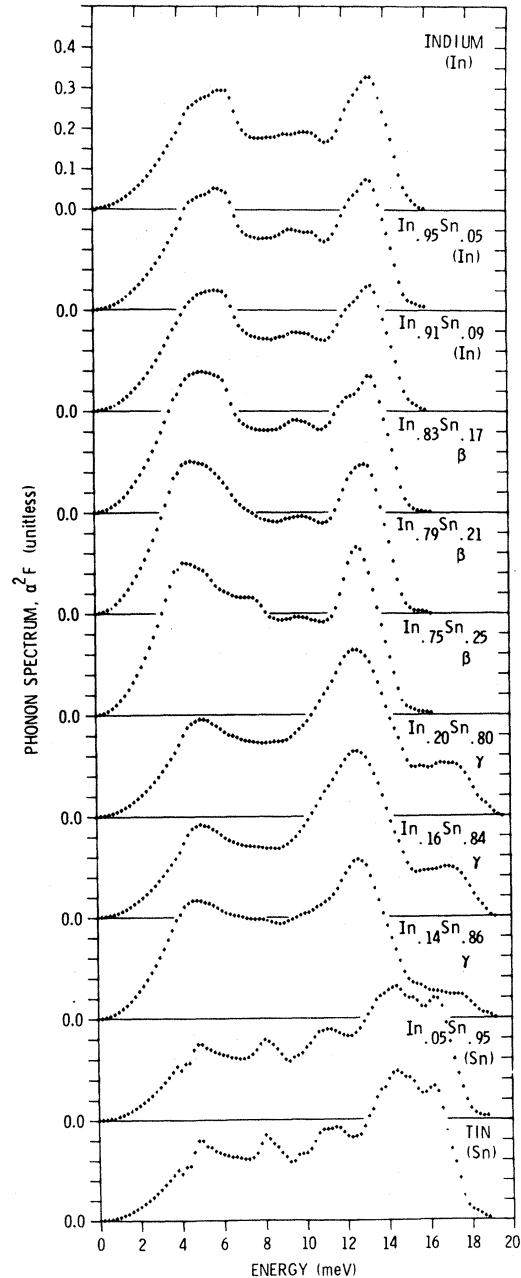


FIG. 8. Phonon spectra [i.e., the product function $\alpha^2(\omega_q)F(\omega_q)$] of the In-Sn system. Traces 1, 2, 3 for the In-like phase, traces 4, 5, 6 for the β phase; traces 7, 8, 9 for the γ phase, and traces 10, 11 for the Sn-like phase.

junctions were stored in liquid N₂ at least three days before recording the tunneling data.

Errors in the $\alpha^2(\omega_q)F(\omega_q)$ data may be associated with the amplitudes and with the energies of the peaks in these traces, Fig. 8. The reference to Rowell *et al.*,⁸ cited above, on the accuracy of the

electron density-of-states-ratio determinations shows that the peak amplitudes of the $\alpha^2(\omega_q)F(\omega_q)$ traces may vary as much as 15%, but, more importantly, the energy levels associated with the peaks fall within ± 0.1 meV of the indicated value.

The spectra in Fig. 8 for pure In and pure Sn are in good agreement with the previously reported spectra.^{7,8} For example the amplitudes of our low- and high-energy peaks for In are within 3.5% of the amplitudes of the low- and high-energy peaks of Dynes.⁷ Our energies for the peaks in the phonon density of states for In agree with those of Dynes within ± 0.1 meV. This conclusion was reached through a comparison of unpublished numerical computer printouts of the data (our data and Ref. 32) used in plotting the phonon spectrum in Fig. 8. A similar comparison was made for Sn. The amplitudes of the six prominent peaks of Rowell *et al.*⁸ agree with our amplitudes within 14.5% and the energies of five of the six peaks in the phonon density of states agree within ± 0.1 meV. The peak nominally occurring at 11.2 meV is in disagreement by ± 0.2 meV. We have a somewhat flatter peak at this energy than that obtained by Rowell *et al.*⁸

We had some doubts about our $\text{In}_{0.14}\text{Sn}_{0.86}$ alloy film because it had a comparatively broad superconducting-to-normal transition range: a ΔT transition equal to 0.5 K as compared with 0.01 K for the other alloy films. A broad transition may indicate a mixture of phases²⁸ or that the film was not completely annealed. Merriam and von Herzen found that the T_c 's of bulk samples in the γ phase varied over a range of 3 K depending on the state of annealing, with the best-annealed specimens having the lowest T_c 's.

In Figs. 9 and 10 are presented the gap-equation solutions of the gap functions [$\Delta(\omega)$, Eq. (3)] for the β and γ phases, respectively. Both the real (solid lines) and imaginary (dashed lines) parts of these functions are graphed. The imaginary parts contribute to (i) a determination of the lifetimes of the electron quasiparticle states, and (ii) the retardation effects in the electron-phonon interaction. It can be seen from Figs. 9 and 10 that the pairing interaction is positive (attractive) at low energies and negative (repulsive) at higher energies, approximately above ω_D .

C. Transition temperatures

The superconducting transition temperatures for the (In), γ , and (Sn) phases of the In-Sn system were directly measured using the tunneling method of Feldman and Rowell.²⁸ The transition temperatures for the γ -phase alloys, all above 4.2 K, were obtained by overpressuring the liquid-He bath. The transition temperatures of the β -phase

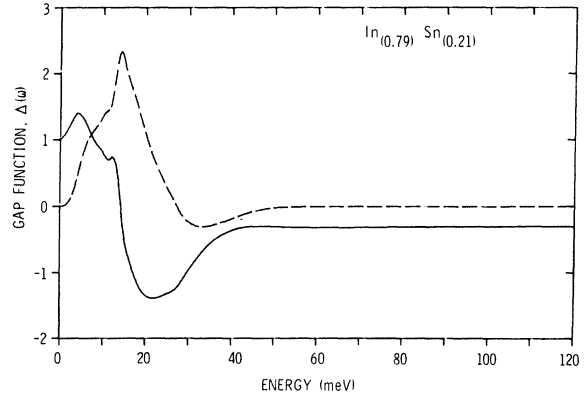


FIG. 9. Superconducting state gap function $\Delta(\omega)$ for an $\text{In}_{0.79}\text{Sn}_{0.21}$ junction, representative of the β phase of the In-Sn system: real part (solid line) and imaginary part (dashed line).

alloys, all above the critical temperature of He, were inaccessible. The measured transition temperatures distinguished by the symbol $T_c(\text{tun})$ are entered in Table II. The uncertainty of the $T_c(\text{tun})$ data is $\sim \pm 0.03$ K.

Values of the normal-state properties A^2 , λ , and $\langle \omega_q \rangle$, derived from the phonon spectra using Eqs. (6)–(9), are entered in Table II. These are used with values of the Coulomb pseudopotential μ^* , also entered in Table II, to compute the superconducting transition temperatures $T_c(\text{McM})$ using the McMillan equation, Eq. (5). Allen and Dynes⁴¹ have shown recently that $T_c(\text{McM})$ values are in good agreement with measured values of T_c for values of $\lambda < 1.5$. All our values of λ were less than 1.2 (Table II). Our $T_c(\text{McM})$ data are listed in Table II together with transition temperatures $T_c(\text{M, vH})$ from the paper by Merriam and von Herzen¹⁰ for well-annealed bulk specimens. Val-

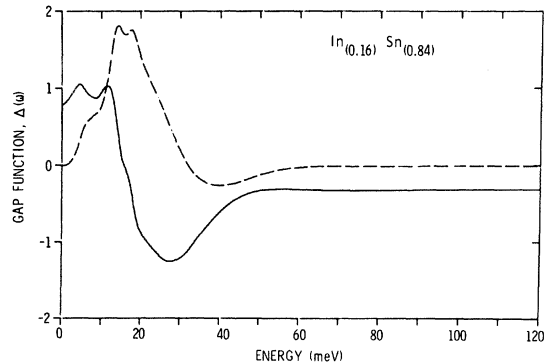


FIG. 10. Superconducting state gap function $\Delta(\omega)$ for an $\text{In}_{0.16}\text{Sn}_{0.84}$ junction, representative of the γ phase of the In-Sn system: real part (solid line) and imaginary part (dashed line).

ues of T_c (M, vH) for our compositions were obtained by linear interpolation between the data points.

Some Table II values for the $\text{In}_{0.14}\text{Sn}_{0.86}$ alloy are not altogether consistent with the values for the other alloys. In Sec. IIIB attention was called to the broad ΔT , superconducting-to-normal transition range, for this alloy film and it was inferred that the film was either a mixture of phases or was not completely annealed. We think this film should be considered as an example of either a mixture of phases or an insufficiently annealed film.

Figure 11 is a plot of the T_c data in Table II. Using the Merriam-von Herzen data in Fig. 11 for reference, the compositions of our alloy films can be determined from our measured transition temperatures T_c (tun). The compositions estimated in this way are lower in Sn content than the admixture compositions of the flash-evaporated pellets by between 1 and 2 at.% on the average. The maximum difference is 3 at.% for the alloy

$\text{In}_{0.16}\text{Sn}_{0.84}$.

T_c (McM) values are sensitive to small changes (experimental errors) in μ^* . Values of T_c computed from the data in Table I in the Rowell, McMillan, and Feldman paper⁸ for five of their Sn-tunnel junctions range from 3.61 to 4.25 K with a mean of 3.89 K and a standard deviation of 0.32 K. The most uncertain of the three parameters (μ^* , λ , $\langle\omega\rangle$) used in the computation of T_c (McM) is μ^* .

It is interesting to compare the changes in the T_c 's of the tetragonally structured (In)- and β -

phase alloys, that result from changes in their composition, with the changes in the T_c 's of the system of binary and tertiary alloys of the Tl-Pb-Bi systems³⁸ when their composition is changed. Figure 11 shows that there is a monotonic increase of T_c with increase of Sn content through the (In) and β phases, in spite of the fact that the phonon spectra, Fig. 8, of (In) and β alloys are so similar. This similarity of phonon spectra is reflected in the small change in $\langle\omega_q\rangle$, see Table II, compared with the change in T_c , as one progresses from pure In to a concentration of 25 at.% of Sn. We believe the increase in T_c implies a strong dependence of T_c on the increase in the conduction-electron/atom ratio as more 4-valent Sn is substituted for 3-valent In. If this is the case, our results for the (In) and β phases are in essential agreement with the results of Dynes and Rowell³⁸ for alloys of the Tl-Pb-Bi system.

V. CONCLUDING REMARKS

A study has been made of the superconducting properties of all four solid-solution single phases of the In-Sn-alloy system making use of the detailed theory of the Eliashberg gap equations. The central result is the first presentation of the In-Sn phonon spectra for each single-phase alloy. The phonon spectra have been shown to reflect differences in crystal structure. The (In) and β phases, both having tetragonal structures with not very different axial ratios (c/a), have similar phonon spectra. The phonon spectra of the γ and (Sn) phases, however, are quite distinctive within their respective phases. The ratios of superconducting, electronic density of quasiparticle states to the BCS density of states are exhibited for the β and γ phases in Figs. 6 and 7.

Transition-temperature measurements on films have been compared with previous measurements on well-annealed bulk specimens. There is good agreement, especially if a little leeway is permitted for some variation of composition with flash evaporation. The reasonably good agreement of the transition temperatures gives added support for the flash-evaporation technique as a reliable means for controlling alloy-film composition. The transition temperatures calculated using the McMillan equation are in good agreement with the transition temperatures measured by the tunneling technique. For the β phase, transition temperatures calculated with the McMillan equation, using our data, are in good agreement with bulk sample, measured T_c 's, and give a high level of confidence to the compositions assigned to the β -phase films.

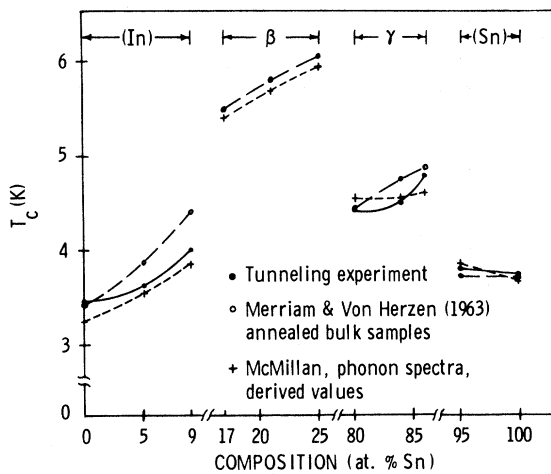


FIG. 11. Comparison of transition temperatures: ● experimental, from tunneling measurements (this investigation); ○ experimental by Merriam and von Herzen (Ref. 10) on annealed bulk specimens; and + calculated using the McMillan equation (5) and data from this investigation.

ACKNOWLEDGMENTS

The authors thank Dr. J. M. Rowell and Dr. R. C. Dynes of the Bell Laboratories, the former for helpful suggestions in the initial phases of the investigation and guidance in the form of selected reprints, and the latter for freely sharing his time with respect to both theoretical and experimental

details, especially with respect to the flash evaporation of alloy films. We are indebted to Professor W. L. McMillan of the University of Illinois for supplying us with his gap-equation computer program listing. One of us (E. L. M.) thanks Professor H. A. Atwater for numerous helpful discussions and critical pieces of apparatus, and, also, Professor P. H. Cutler for enlightening discussions.

-
- *Present address: Marine Systems Division, Rockwell International, Arlington, Va. 22202.
- ¹I. Giaever, Phys. Rev. Lett. 5, 147 (1960).
- ²I. Giaever and K. Megerle, Phys. Rev. 122, 1101 (1961).
- ³J. R. Schrieffer, D. J. Scalapino, and J. W. Wilkins, Phys. Rev. Lett. 10, 336 (1963).
- ⁴J. M. Rowell, P. W. Anderson, and D. E. Thomas, Phys. Rev. Lett. 10, 334 (1963).
- ⁵W. L. McMillan and J. M. Rowell, Phys. Rev. Lett. 14, 108 (1965).
- ⁶G. M. Eliashberg, Zh. Eksp. Teor. Fiz. 38, 966 (1960) [Sov. Phys.-JETP 11, 696 (1960)].
- ⁷R. C. Dynes, Phys. Rev. B 2, 644 (1970).
- ⁸J. M. Rowell, W. L. McMillan, and W. L. Feldman, Phys. Rev. B 3, 4065 (1971).
- ⁹F. A. Shunk, *Constitution of Binary Alloys, Second Supplement* (McGraw-Hill, New York, 1969).
- ¹⁰M. F. Merriam and M. von Herzen, Phys. Rev. 131, 637 (1963).
- ¹¹R. C. Dynes, J. P. Carbotte, D. W. Taylor, and C. K. Campbell, Phys. Rev. 178, 713 (1969).
- ¹²R. C. Dynes and J. M. Rowell, Phys. Rev. 187, 821 (1969).
- ¹³W. L. McMillan and J. M. Rowell, in *Superconductivity*, edited by R. D. Parks (Dekker, New York, 1969), Chap. 11.
- ¹⁴J. Bardeen, L. N. Cooper, and J. R. Schrieffer, Phys. Rev. 108, 1175 (1957).
- ¹⁵Y. Nambu, Phys. Rev. 117, 648 (1960).
- ¹⁶J. R. Schrieffer, *Theory of Superconductivity* (Benjamin, Reading, Mass., 1964).
- ¹⁷D. J. Scalapino, in Ref. 13, Chap. 10.
- ¹⁸P. Morel and P. W. Anderson, Phys. Rev. 125, 1263 (1962).
- ¹⁹J. M. Rowell, W. L. McMillan, and W. L. Feldman, Phys. Rev. 178, 897 (1969).
- ²⁰W. L. McMillan, Phys. Rev. 167, 331 (1968).
- ²¹V. Ambegaokar and L. Tewordt, Phys. Rev. 134, A805 (1964).
- ²²D. J. Scalapino, Y. Wada, and J. C. Swihart, Phys. Rev. Lett. 14, 102 (1965).
- ²³J. L. Miles and P. H. Smith, J. Electrochem. Soc. 110, 1240 (1963).
- ²⁴J. Vrba and S. B. Woods, Can. J. Phys. 50, 548 (1972).
- ²⁵J. G. Adler and J. E. Jackson, Rev. Sci. Instrum. 37, 1049 (1966).
- ²⁶D. E. Thomas and J. M. Rowell, Rev. Sci. Instrum. 36, 1301 (1965).
- ²⁷A. F. Hebard and P. W. Shumate, Rev. Sci. Instrum. 45, 529 (1974).
- ²⁸W. L. Feldman and J. M. Rowell, J. Appl. Phys. 40, 312 (1969).
- ²⁹W. H. Hubin, Tech. Rep. No. 182, Dept. of Physics, University of Illinois, Urbana, Ill., 1970 (unpublished).
- ³⁰J. R. Schrieffer, in *Tunneling Phenomena in Solids*, edited by E. Burstein and S. Lundqvist (Plenum, New York, 1969), Chap. 21.
- ³¹The method of adjusting $\alpha^2F^{(c)}$ is described on pp. 594 and 595 of McMillan's and Rowell's paper (Ref. 13).
- ³²J. M. Rowell, W. L. McMillan, and R. C. Dynes (unpublished).
- ³³J. G. Adler and J. S. Rogers, Phys. Rev. Lett. 10, 217 (1963).
- ³⁴J. G. Adler, J. S. Rogers, and S. B. Woods, Can. J. Phys. 43, 557 (1965).
- ³⁵M. Hansen, *Constitution of Binary Alloys* (McGraw-Hill, New York, 1958).
- ³⁶L. Y. L. Shen, Phys. Rev. Lett. 29, 1082 (1972).
- ³⁷Roger W. Cohen, AIP Conf. Proc. 4, 144 (1972).
- ³⁸R. C. Dynes and J. M. Rowell, Phys. Rev. B 11, 1884 (1975).
- ³⁹R. W. Wyckoff, *Crystal Structures*, 2nd ed. (Interscience, New York, 1963).
- ⁴⁰W. B. Pearson, *Lattice Spacings and Structure of Metals and Alloys* (Pergamon, New York, 1958).
- ⁴¹P. B. Allen and R. C. Dynes, Phys. Rev. B 12, 905 (1975).